

In Vivo Target Sites of Nitric Oxide in Photosynthetic Electron Transport as Studied by Chlorophyll Fluorescence in Pea Leaves^{1[OA]}

Barnabás Wodala, Zsuzsanna Deák, Imre Vass, László Erdei, István Altorjay, and Ferenc Horváth*

Department of Plant Physiology, University of Szeged, H-6701 Szeged, Hungary (B.W., L.E., F.H.); Institute of Plant Biology, Biological Research Center of the Hungarian Academy of Sciences, H-6701 Szeged, Hungary (Z.D., I.V.); and Department of Gastroenterology, Medical and Health Science Centre, University of Debrecen, H-4001 Debrecen, Hungary (I.A.)

The role of nitric oxide (NO) in photosynthesis is poorly understood as indicated by a number of studies in this field with often conflicting results. As various NO donors may be the primary source of discrepancies, the aim of this study was to apply a set of NO donors and its scavengers, and examine the effect of exogenous NO on photosynthetic electron transport in vivo as determined by chlorophyll fluorescence of pea (*Pisum sativum*) leaves. Sodium nitroprusside-induced changes were shown to be mediated partly by cyanide, and *S*-nitroso-*N*-acetylpenicillinamine provided low yields of NO. However, the effects of *S*-nitrosoglutathione are inferred exclusively by NO, which made it an ideal choice for this study. Q_A^- reoxidation kinetics show that NO slows down electron transfer between Q_A and Q_B , and inhibits charge recombination reactions of Q_A^- with the S_2 state of the water-oxidizing complex in photosystem II. Consistent with these results, chlorophyll fluorescence induction suggests that NO also inhibits steady-state photochemical and nonphotochemical quenching processes. NO also appears to modulate reaction-center-associated nonphotochemical quenching.

Plants, as well as animals, respond to ambient levels of nitric oxide (NO), and also generate NO themselves via various enzymatic and nonenzymatic pathways (Yamasaki, 2000; Neill et al., 2003; Río et al., 2004). Indeed, in the past years, a growing amount of research has provided evidence for the multiple physiological roles of this gaseous free radical in plants (for review, see Wendehenne et al., 2004; Delledonne, 2005). The turnover of NO depends on its concentration, the ambient redox status, and the concentration of target molecules. In biological systems, NO is capable of targeting thiol- and metal-containing proteins (Lamattina et al., 2003). Photosynthetic and mitochondrial electron transport chains are abundant in transition metal-containing complexes, and NO and its derivative peroxy-nitrite are known to inhibit the mitochondrial electron transport chain (Millar and Day, 1996; Yamasaki et al.,

2001). Yet, the effect of exogenous NO on photosynthetic activity in intact leaves has so far been poorly addressed, with often conflicting results.

Previous research suggests that NO gas decreases net photosynthesis rates in oat (*Avena sativa*) and alfalfa (*Medicago sativa*) leaves (Hill and Bennett, 1970). Lum et al. (2005) have identified a number of intracellular targets of NO signalization including mitochondria, peroxisomes, and chloroplasts. They found that the NO donor sodium nitroprusside (SNP) decreases the amount of Rubisco activase and the β -subunit of the Rubisco subunit-binding protein in mung bean (*Phaseolus aureus*).

NO is also able to influence the photosynthetic electron transport chain directly. An important action site of NO is PSII. Electron paramagnetic resonance and chlorophyll fluorescence measurements using NO gas treatment of isolated thylakoid membrane complexes have clearly demonstrated that NO can reversibly bind to several sites in PSII and inhibit electron transfer. Important binding sites of NO within the PSII complex are the nonheme iron between Q_A and Q_B binding sites (Diner and Petrouleas, 1990), the Y_D Tyr residue of the D2 protein (Sanakis et al., 1997), and the manganese (Mn) cluster of the water-oxidizing complex (Schansker et al., 2002).

Takahashi and Yamasaki (2002) showed that the NO donor *S*-nitroso-*N*-acetylpenicillinamine (SNAP) does not modify the maximal quantum efficiency (F_v/F_m), but inhibits the linear electron transport rate, ΔpH formation across the thylakoid membrane, and decreases the rate of ATP synthesis. Yang et al. (2004) measured the chlorophyll fluorescence of intact potato

¹ This work was supported by the Hungarian Scientific Research Fund (grant nos. OTKA F 048787 and OTKA T 048436), the National Research and Development Programme (grant no. NKFP 3A/009/2004), the Economic Competitiveness Operative Programme (grant no. GVOP-3.2.1-2004-04-0419/3.0), the Poland and Hungary Action for Restructuring of the Economy (grant no. PHARE HU2003/005.830.01-04), and the European Union (grant no. MRTN-CT-2003-505069).

* Corresponding author; e-mail horvathf@bio.u-szeged.hu.

The author responsible for distribution of materials integral to the findings presented in this article in accordance with the policy described in the Instructions for Authors (www.plantphysiol.org) is: Ferenc Horváth (horvathf@bio.u-szeged.hu).

[OA] Open Access articles can be viewed online without a subscription.

www.plantphysiol.org/cgi/doi/10.1104/pp.107.110205

Table I. Concentration of NO (μM) generated by various NO donors

Concentration of NO generated by photolytic decomposition of NO donors at the end of a 2-h white light treatment. One-micromolar aqueous solutions of SNP, GSNO, and SNAP were assayed, and PTIO and Hb scavengers were used in concentrations of 1 mM and 4 mg mL⁻¹, respectively. Light intensity was 150 $\mu\text{mol m}^{-2} \text{s}^{-1}$. Values represent means \pm SD ($n = 4$).

SNP	SNP + PTIO	GSNO	GSNO + PTIO	GSNO + Hb	SNAP
0.78 \pm 0.06	0.10 \pm 0.06	2.70 \pm 0.62	0.10 \pm 0.03	0.47 \pm 0.20	0.48 \pm 0.16

(*Solanum tuberosum*) leaves treated with SNP, but did not observe any differences in ΔpH -dependent non-photochemical quenching (NPQ). They found, however, that SNP decreases F_v/F_m values in a concentration-dependent manner.

The aim of this work was to resolve previous contradictory results concerning the effect of exogenous NO on photosynthetic electron transport in intact leaves using three different NO donors. We show that S-nitrosoglutathione (GSNO) is the most suitable to study the effect of NO on photosynthetic electron transport, as SNP-induced changes are mediated partly by cyanide (CN⁻), the by-product of its degradation; and SNAP shows modest effects due to its low yields of NO under our experimental conditions. Using GSNO, target sites of NO at both the donor and acceptor sides of PSII are identified.

RESULTS

NO Donor Molecules Release Different Amounts of NO

Excised pea (*Pisum sativum*) leaf discs were incubated in covered, but not sealed petri dishes with NO donor and scavenger solutions for 2 h under 150 $\mu\text{mol m}^{-2} \text{s}^{-1}$ white light. These conditions provided homogenous light treatment, thus avoiding potential illumination-related differences in chlorophyll fluorescence parameters.

Using a NO electrode, the concentration of NO released by the photochemical degradation of NO donors was determined after 2 h incubation under 150 $\mu\text{mol m}^{-2} \text{s}^{-1}$ white light (Table I). One millimolar GSNO produced the highest NO concentration with values above 2.5 μM , while 1 mM SNP and 1 mM SNAP solutions contained less than 1 μM NO. The potassium salt of 2-phenyl-4,4,5,5-tetramethylimidazoline-1-oxyl-3-oxide (PTIO) successfully scavenged almost all NO released by GSNO and SNP; and hemoglobin (Hb), another NO scavenger, also eliminated considerable amounts of GSNO-derived NO. Monitoring the NO emission of NO donor solutions reveals that SNAP releases the bulk of its NO content in the first hour of the incubation, leading to residual amounts of NO after 2 h, while SNP and GSNO both yield significant amounts of NO even after 2 h illumination (data not shown). This trend is comparable with previous results on NO release kinetics from these NO donors (Floryszak-Wieczorek et al., 2006), and is consistent

with earlier reports on the shorter half-life of SNAP (Feelisch, 1998).

In accordance with the small NO concentration in 1 mM SNAP solution after 2 h incubation, 1 mM SNAP caused no significant changes in either Q_A^- reoxidation kinetics, or chlorophyll fluorescence parameters (data not shown); therefore, SNAP is an unsuitable NO donor under our conditions.

SNP, on the other hand, produced larger amounts of NO after 2 h incubation, and significantly altered chlorophyll fluorescence parameters. F_v/F_m and photochemical quenching (qP) values of leaf discs incubated for 2 h at 150 $\mu\text{mol m}^{-2} \text{s}^{-1}$ in 200 μM SNP decreased from 0.82 to 0.53 and from 0.87 to 0.39, respectively, in agreement with Yang et al. (2004). However, the interpretation of SNP-mediated effects is challenging because SNP releases CN⁻ as well as nitrosonium cation during its photolysis (Feelisch, 1998; Lum et al., 2005). It has previously been reported that CN⁻ affects F_v/F_m (Jones et al., 1999) and may well affect additional chlorophyll fluorescence parameters, because CN⁻ is known to inhibit photosynthesis at various levels. At submillimolar concentrations, CN⁻ inhibits Rubisco (Wishnick and Lane, 1969) and ascorbate peroxidase (Forti and Gerola, 1977), leading to hydrogen peroxide accumulation, which interacts

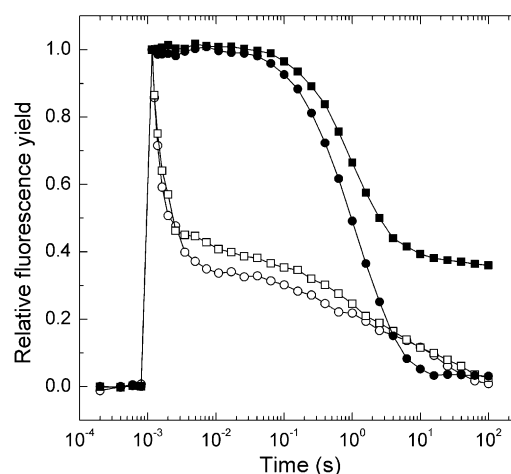


Figure 1. The effect of NO on fluorescence decay kinetics. Measurements were carried out on leaf discs that were incubated for 2 h under 150 $\mu\text{mol m}^{-2} \text{s}^{-1}$ white light in distilled water (circles), 1 mM GSNO (squares), then dark adapted for 15 min with (black symbols) or without (white symbols) incubation in 100 μM DCMU. Curves are normalized to the same amplitude and each trace is the average of four measurements.

Table II. Decay kinetics of flash-induced variable fluorescence

Analysis of the fluorescence relaxation kinetics. Measurements were performed on leaf discs, as in Figure 1, that were incubated for 2 h under $150 \mu\text{mol m}^{-2} \text{s}^{-1}$ white light in distilled water (control), or solutions containing NO donor and scavenger chemicals, each used in 1 mM concentration, then dark adapted for 15 min with or without incubation in $100 \mu\text{M}$ DCMU. The curves were analyzed in terms of two exponential components (fast and middle phases) and one hyperbolic component (slow phase). Values in parentheses are relative amplitudes as a percentage of total variable fluorescence. SES of the calculated parameters are also indicated.

Treatment	Fast Phase τ_1 (A_1 [%])	Middle Phase τ_2 (A_2 [%])	Slow Phase τ_3 (A_3 [%])	A_0
	μs	ms	s	%
	Without DCMU			
Control	800 ± 40 (51 ± 1.4)	194 ± 31 (14 ± 0.9)	10.5 ± 0.8 (35 ± 0.8)	0
GSNO	790 ± 50 (45 ± 1.4)	430 ± 62 (18 ± 1.4)	11.7 ± 2.1 (35 ± 1.3)	1.8 ± 1.4
GSNO + PTIO	720 ± 40 (45 ± 1.5)	312 ± 44 (17 ± 1.1)	9.4 ± 0.8 (38 ± 1.1)	0
	With DCMU			
Control	– (0)	– (0)	1.6 ± 0.1 (100 ± 0.4)	0
GSNO	– (0)	– (0)	1.2 ± 0.1 (49 ± 0.6)	51 ± 0.5
GSNO + PTIO	– (0)	– (0)	2.5 ± 0.1 (73 ± 0.7)	27 ± 0.6

with the light activation of Calvin cycle enzymes (Kaiser, 1979). CN^- also hinders electron transfer in PSII by competing with bicarbonate at the $Q_A\text{Fe}^{2+}Q_B$ complex (Goussias et al., 2002). Indeed, applying 1 mM PTIO only partially restored the SNP-induced changes in F_v/F_m and qP values: to 0.68 and 0.63, respectively, which suggests that CN^- and NO are both responsible for the effect of SNP. To provide direct evidence for a CN^- effect, $200 \mu\text{M}$ SNP was substituted with 1 mM potassium CN^- , as SNP may release up to five CN^- molecules per SNP molecule (Friederich and Butterworth, 1995). F_v/F_m and qP values of leaf discs treated with 1 mM CN^- decreased to 0.73 and 0.69, respectively, which is strikingly similar to results obtained in the presence of $200 \mu\text{M}$ SNP and 1 mM PTIO. Therefore, SNP is also a highly unsuitable NO donor for studies on photosynthesis.

Besides NO release, the photolysis of GSNO yields oxidized glutathione (GSSG), which may influence chlorophyll fluorescence parameters. GSSG potentially interferes with redox signaling processes in the chloroplast, such as the ferredoxine-thioredoxin pathway involved in the regulation of carbon fixation enzymes (Michelet et al., 2005). In addition, reduced glutathione has been shown to interfere with the NPQ mechanism by inhibiting violaxanthin deepoxidation, although the inhibition is weak, as reduced glutathione caused no significant inhibition at 2.5 mM (Xu et al., 2000). Michelet et al. (2005) have shown that 5 h incubation with 5 mM GSSG leads to glutathionylation of thioredoxin f, a key factor in the regulation of carbon fixation enzymes, which impairs light activation of the Calvin cycle, and such an effect may lead to altered chlorophyll fluorescence parameters. To rule out the possibility of a potential GSSG effect, we measured chlorophyll fluorescence parameters of leaf discs incubated for 2 h under $150 \mu\text{mol m}^{-2} \text{s}^{-1}$ white light in petri dishes containing 0.5 mM GSSG, but found no effect (data not shown).

In aqueous solutions, NO may rapidly react with water and oxygen to form nitrite (NO_2^-) and nitrate anions (Takahashi and Yamasaki, 2002). NO can also

react with oxygen in the air and form nitrogen dioxide, a well-known photosynthetic inhibitor (Yamasaki, 2000) whose toxic effects are probably mediated by NO_2^- , as nitrogen dioxide forms NO_2^- when entering aqueous solutions (Wellburn, 1990). Incubating leaf discs for 2 h in a mixture of $200 \mu\text{M}$ sodium nitrite and sodium nitrate showed no effects on the examined photosynthetic parameters (data not shown). This finding rules out the possibility of effects mediated by degradation products of NO under our conditions.

NO Causes Donor and Acceptor Side Inhibition of PSII Electron Transport in Vivo

To investigate the inhibitory effect of NO on donor and acceptor side electron transfer, we measured Q_A^- reoxidation kinetics of leaf discs incubated in a solution containing GSNO with or without the specific NO scavenger PTIO. A short saturating light pulse reduces Q_A^- causing a rapid increase in fluorescence yield,

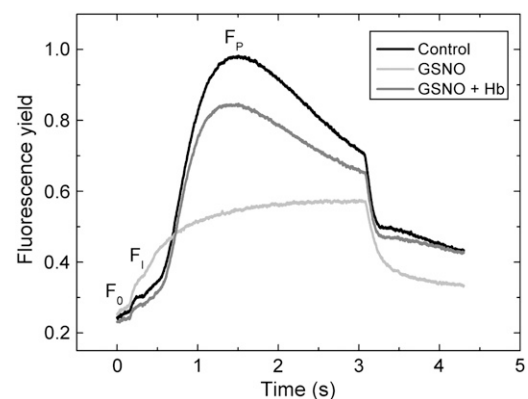


Figure 2. The effect of NO on fluorescence induction kinetics. Leaf discs were incubated for 2 h under $150 \mu\text{mol m}^{-2} \text{s}^{-1}$ white light in distilled water (Control), 1 mM GSNO, and 1 mM GSNO + 4 mg mL^{-1} Hb, then dark adapted for 15 min. Following this treatment, chlorophyll fluorescence of leaf discs was induced by 3 s of $130 \mu\text{mol m}^{-2} \text{s}^{-1}$ red light. Curves show the average of five measurements each.

Table III. Fast fluorescence induction parameters

Fast fluorescence induction parameters of curves in Figure 3. Leaf discs were incubated for 2 h under $150 \mu\text{mol m}^{-2} \text{s}^{-1}$ white light in distilled water (control), 1 mM GSNO, and 1 mM GSNO + 4 mg mL^{-1} Hb, then dark adapted for 15 min. Following this treatment, chlorophyll fluorescence of leaf discs was induced by 3 s of $130 \mu\text{mol m}^{-2} \text{s}^{-1}$ red light. The F_0 , F_1-F_0 , and F_p-F_0 parameters are shown in arbitrary units. Values represent means \pm SD ($n = 5$).

Treatment	F_0	F_1-F_0	F_p-F_0	Slope of Curve (F_1-F_p)
Control	258.3 ± 4.6	46.3 ± 7.6	727.0 ± 6.0	1.1 ± 0.01
GSNO	270 ± 6.1	88.0 ± 6.9	309.3 ± 13.3	0.3 ± 0.04
GSNO + Hb	240.0 ± 10.8	39.7 ± 10.8	616.7 ± 38.5	1.1 ± 0.02

followed by a decay in the subsequent dark period due to Q_A^- reoxidation. Curves from untreated samples are characterized by a fast (approximately 800 μs), middle (approximately 190 ms), and a slow (approximately 10 s) phase (Fig. 1). GSNO caused no significant changes in either the time constants (τ) or the amplitude values (A) of the fast phase in accordance with Diner and Petrouleas (1990), who observed inhibition after the second flash only. In the middle phase, 1 mM GSNO increased the time constants to approximately 430 ms. In the presence of the specific NO scavenger PTIO, this increase is reduced to 310 ms (Table II). GSNO increased the amplitude of the middle phase, but the addition of PTIO led only to a minor reversal of this effect. The slower time constant of the middle phase suggests that NO inhibits the binding of plastoquinone (PQ) molecules at the Q_B binding site, while the increasing amplitude indicates a reduced amount of Q_B binding sites occupied by PQ at the time of the flash following the NO donor treatment.

When Q_A^- reoxidation via forward electron transport is inhibited by 3-(3,4-dichlorophenyl)-1,1-dimethylurea (DCMU), which occupies the Q_B binding site, the fast and middle phases of the fluorescence decay curve are converted to a slow phase with approximately 2 s time constant, which reflects Q_A^- reoxidation via charge recombination with the S_2 state of the water-oxidizing complex. In the presence of DCMU, a significant fraction of fluorescence does not decay in the GSNO-treated leaf discs (Fig. 1). This effect is largely prevented in the presence of PTIO (Table II). The increase in the nondecaying part of fluorescence correlates with previous results of Schansker et al. (2002) showing that NO reduces the Mn cluster of the water-oxidizing complex into the S_2 state. Our measurements with GSNO indicate that Q_A^- is unable to recombine with the S_2 state, possibly because NO inactivates or reduces the Mn cluster.

Fluorescence Induction Kinetics Indicates Donor and Acceptor Side Inhibition of PSII

Effects of NO on donor and acceptor side of PSII were further investigated by fluorescence induction measurements. Following incubation with GSNO, leaf discs were dark adapted, then a Kautsky curve was measured in which chlorophyll fluorescence yield rises from a minimal level (F_0) through a local mini-

mum (F_1) to a peak value (F_p ; Lichtenthaler, 1992). GSNO treatment caused a 2-fold F_1 increase, indicating inhibition of forward electron transfer at the acceptor side of PSII due to a growing fraction of centers that could only reduce Q_B slowly. F_p decreased to 43% of the control value, but no significant changes were observed in F_0 (Fig. 2). The maximal slope of the F_1-F_p curve was also decreased by GSNO, and this effect was largely restored by the addition of 4 mg mL^{-1} Hb (Table III). The decrease of F_p and the slope of the F_1-F_p curve indicate inhibition of electron transport at the donor side of PSII.

Effect of NO on Chlorophyll Fluorescence Parameters

Following the 2-h incubation in 1 mM GSNO with or without Hb, F_v/F_m , steady-state qP, and NPQ parameters were determined. GSNO reduced F_v/F_m and qP values, which were restored in the presence of Hb (Fig. 3). The results are in good correlation with fluorescence decay kinetics measurements, which indicate an accumulation of the reduced form of the electron acceptor Q_A^- .

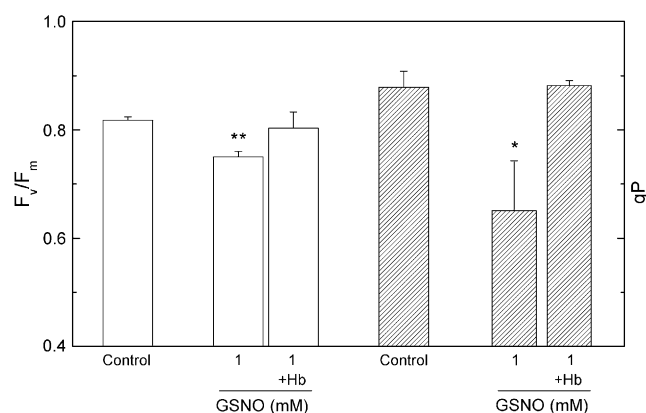


Figure 3. The effect of GSNO on F_v/F_m and on steady-state qP. Prior to measurements, leaf discs were incubated for 2 h under $150 \mu\text{mol m}^{-2} \text{s}^{-1}$ white light in distilled water (Control) and 1 mM GSNO solution, then dark adapted for 15 min. The NO scavenger Hb was applied at a concentration of 4 mg mL^{-1} . Steady-state qP values were recorded at the end of a 30-min $130 \mu\text{mol m}^{-2} \text{s}^{-1}$ red actinic illumination. Bars represent means \pm SD ($n = 4$). Asterisks indicate levels of significance: $P < 0.05$ (*) and $P < 0.01$ (**).

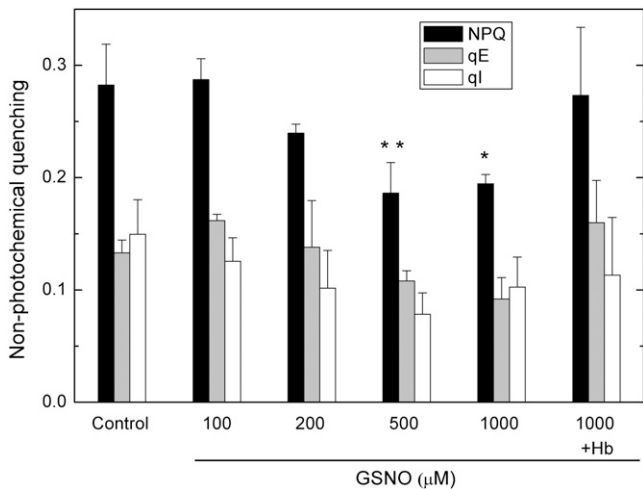


Figure 4. The effect of GSNO on steady-state NPQ. Prior to measurements, leaf discs were incubated for 2 h under $150 \mu\text{mol m}^{-2} \text{s}^{-1}$ white light in distilled water (Control) and GSNO solutions with different concentrations, then dark adapted for 15 min. Hb was applied at a concentration of 4 mg mL^{-1} . Steady-state NPQ values were recorded at the end of a 30-min $130 \mu\text{mol m}^{-2} \text{s}^{-1}$ red actinic illumination. Bars represent means \pm SD ($n = 4$). Asterisks indicate levels of significance: $P < 0.05$ (*) and $P < 0.01$ (**).

The rate of light-dependent acidification of the lumen depends on the rate of electron transport and also on the activity of ATP synthase. The NO-derived inhibition of linear electron transport should reduce proton accumulation in the lumen, which would then cause a decrease in NPQ via the energy-dependent quenching (qE) component. GSNO decreased steady-state NPQ, as well as qE and photoinhibitory quenching components in a concentration-dependent manner (Fig. 4), and this effect is eliminated by Hb. Besides decreasing steady-state NPQ, GSNO changed the length and amplitude of an NPQ transient (Fig. 5A), which resembles the reaction-center NPQ described by Finazzi et al. (2004) in barley (*Hordeum vulgare*) leaves. Figure 5B shows the linear correlation between the increase of the amplitude of NPQ transients and the decrease in the effective quantum efficiency (Φ_{PSII}) in response to growing concentrations of GSNO, which indicates that an increasing proportion of reaction centers switch from photochemistry to heat dissipation.

DISCUSSION

The Choice of NO Donor for Chlorophyll Fluorescence Measurements in Vivo

The use of NO donors is a general tool for investigating the biological roles of NO, but the diverse chemical properties of donors potentially lead to differences in NO yield and the release of other reactive agents. These factors, together with difficulties of direct measurement of NO, may well account for the differences reported in the amounts of NO released by specific NO donors (Delledonne, et al., 1998, 2001;

Lum et al., 2005). Our direct NO measurements clearly demonstrate the differences in NO production of SNAP, GSNO, and SNP (Table I). Measuring leaf discs treated with CN^- , or SNP with or without PTIO shows that SNP releases CN^- , which modifies the chlorophyll fluorescence parameters. The low NO yield of SNAP, and CN^- emission of SNP make both NO donors unsuitable for our studies. On the other hand, our experiments demonstrate that the effects caused by GSNO are inferred by NO exclusively.

NO Hinders Electron Transfer in PSII in Vivo

The terminal electron acceptor in PSII is the linear $\text{Q}_\text{A}\text{Fe}^{2+}\text{Q}_\text{B}$ complex, where Q_A and Q_B can take up one and two electrons, respectively. The rate of electron transfer between the two quinones depends on the coordinative properties of the nonheme iron (II) that, under normal circumstances, forms coordinate covalent bonds with four His residues provided by the D1 and D2 reaction center subunits, as well as one bicarbonate

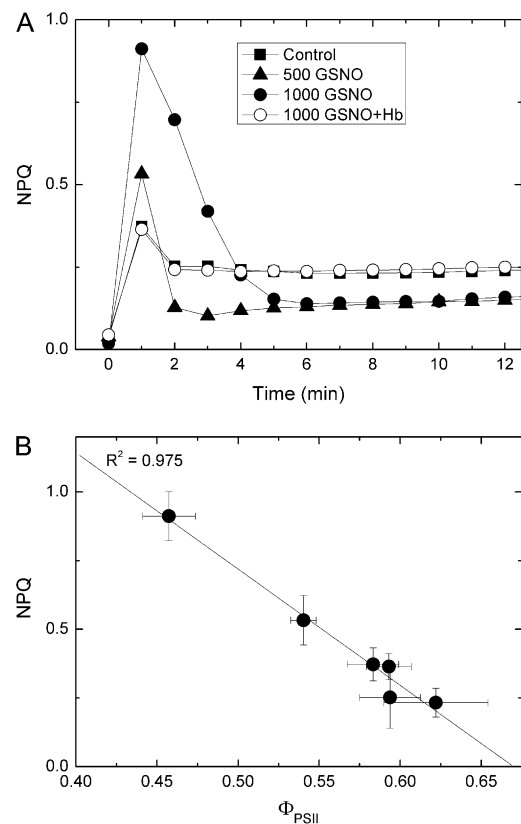


Figure 5. The effect of GSNO on NPQ transient. Prior to measurements, leaf discs were incubated for 2 h under $150 \mu\text{mol m}^{-2} \text{s}^{-1}$ white light in distilled water (Control), and 500 and 1,000 μM GSNO solutions, then dark adapted for 15 min. Hb was applied at a concentration of 4 mg mL^{-1} . During measurements, leaf discs were illuminated with $130 \mu\text{mol m}^{-2} \text{s}^{-1}$ red actinic light. Data are presented as mean \pm SD ($n = 4$). A, Time-dependent change of NPQ. B, Relationship between the amplitude of NPQ and the corresponding effective quantum efficiency values.

occupying one of the remaining two coordination places (Petrouleas and Diner, 1990; Kern et al., 2005). NO and other small molecules, such as CN^- and fluoride anions, compete with bicarbonate and bind reversibly to the nonheme iron (II) (Goussias et al., 2002). Experiments with isolated thylakoids indicate that NO binding slows down the rate of electron transfer between Q_A and Q_B (Diner and Petrouleas, 1990). Binding of NO to the $Q_A\text{Fe}^{2+}Q_B$ complex is facilitated in the presence of reduced Q_A^- acceptor, as this reduction weakens the bond between bicarbonate and iron (Goussias et al., 2002). The rate of electron transport may decrease on the donor side as well, since in vitro experiments have proven that NO interacts with the Y_D Tyr residue and the water-oxidizing complex. The latter is reduced to the S_{-2} state by NO, as shown by oxygen electrode, fluorescence, and electron paramagnetic resonance measurements (Schansker et al., 2002).

Our Q_A^- reoxidation measurements show a reduced rate of electron transport between Q_A and Q_B upon NO donor treatment. This result provides circumstantial evidence in support for the competitive binding of NO to the nonheme iron in vivo (Fig. 1; Table II). Measurements in the presence of DCMU show NO induced inhibition of Q_A^- recombination with the S_2 state of the water-oxidizing complex. This donor side inhibition of electron transport may sufficiently be accounted for by the reduction of either the water-oxidizing complex, or the Y_D residue by NO. Fast chlorophyll fluorescence induction kinetics of GSNO-treated leaf discs confirm significant donor and acceptor side inhibition of electron transport (Fig. 2; Table III).

Effects of NO on Chlorophyll Fluorescence Parameters

Previous chlorophyll fluorescence studies have provided controversial results on changes induced by NO. In isolated chloroplasts, NO derived from SNAP did not affect F_v/F_m ; while in intact leaves, SNP-derived NO decreased its values considerably (Takahashi and Yamasaki, 2002; Yang et al., 2004). However, in both cases, the NO donor treatment caused a decrease in Φ_{PSII} , which is related to qP changes. Our measurements indicate that the different chemical properties of NO donors and different experimental conditions jointly account for previous conflicting results. GSNO caused a significant decrease in F_v/F_m values in intact leaves and decreased steady-state qP, which indicates that NO increases the proportion of closed PSII reaction centers (Fig. 3). Taken together, these data provide strong in vivo evidence that a partial inhibition of PSII by NO is indeed the cause of impaired steady-state electron transport in vivo.

Besides reducing steady-state NPQ values, NO changes the amplitude and kinetics of an NPQ transient (Fig. 5A), which resembles reaction-center NPQ described by Finazzi et al. (2004). Reaction-center NPQ arises upon the onset of illumination of dark-adapted leaves and, at low light intensities, it is relaxed rapidly

after a few minutes of illumination. On the basis of its fast relaxation and ΔpH dependency, Finazzi et al. (2004) showed that reaction-center NPQ is caused by the rapid and transient overacidification of the thylakoid lumen, which is created by the immediate onset of photochemistry. In addition, they suggest that the ΔpH may be further increased by cyclic and pseudo-cyclic electron transport (Mehler reaction) and explain the relaxation of this transient form of NPQ by the activation of the carbon fixation apparatus, which decreases ΔpH and redox pressure. Although a potential effect of NO on Calvin cycle activation would account for changes in this NPQ transient, steady-state NPQ values below control values indicate that NO does not decrease the maximum rate of the Calvin cycle. Further investigations are therefore necessary to clarify the mechanism through which NO modifies the NPQ transient.

CONCLUSION

In conclusion, this study tested an array of NO donors and scavenger chemicals on intact leaves and demonstrated that the SNP-induced changes are mediated partly by CN^- and that a 2-h incubation leads to low NO yields from SNAP, while the biological effect of GSNO is related to NO exclusively. This underlines the importance of data interpretation and adequate choice of NO donor, and justifies the use of GSNO to study the effect of NO on photosynthetic electron transport in vivo. Measurements with GSNO provide in vivo confirmation of target sites of NO in PSII and further evidence on the inhibitory effect of NO on photosynthetic electron transport in intact leaves. In addition, NO was shown to modulate reaction-center-associated NPQ. Taken together, these findings confirm previous in vitro data and offer promising perspectives for NO as a potential regulator of photosynthetic electron transport yet to be discovered.

MATERIALS AND METHODS

Chemicals

The NO donors GSNO, SNP, and SNAP were purchased from Sigma-Aldrich. The NO scavengers Hb and the potassium salt of PTIO were purchased from Sigma-Aldrich. The electron transport inhibitor DCMU was purchased from ICN Biomedicals Inc. Standard chemicals of analytical grade were from Sigma-Aldrich.

Plant Material and Experimental Solutions

Sterilized seeds of pea (*Pisum sativum* 'Petit Provençal') were germinated for 3 d at 24°C, and the seedlings were grown in a semicontrolled growth chamber for 2 weeks under a 12-h-light ($150 \mu\text{mol m}^{-2} \text{s}^{-1}$)/12-h-dark cycle and temperature of 22°C. Leaf discs of the youngest fully expanded leaves were prepared by a 15 mm diameter leaf punch and used for each measurement. Prior to measurements, leaf discs were individually incubated for 2 h under $150 \mu\text{mol m}^{-2} \text{s}^{-1}$ white light in covered petri dishes, which were 10 mm deep and 36 mm in diameter, then dark adapted for 15 min. During the incubation, leaf discs were floating in the covered but not sealed petri dishes containing 4 mL of distilled water as control, or 4 mL of different dilutions of NO donor molecules and scavenger chemicals in aqueous solution. The

volume of the aqueous phase left an approximately 6 cm³ upper ambient space in the covered petri dishes.

GSNO, SNP, and SNAP were used as NO donors, and Hb and PTIO were applied as NO scavengers. Some measurements were conducted in the presence of 100 μM DCMU. To increase their stability, thus preventing an early and unwanted NO release, SNP, SNAP, and GSNO stock solutions were prepared daily and kept in dark on ice until the start of experiments (Singh et al., 1996; Feelisch, 1998).

NO Measurements

Solutions of NO donors with or without scavengers were incubated in petri dishes in the same way as leaf discs, and the amount of NO released at the end of the 2-h incubation under 150 μmol m⁻² s⁻¹ white light was measured using a NO electrode (ISO-NOP; World Precision Instruments Inc.) dipped in the stirred aqueous phase. The NO electrode was calibrated by adding different volumes of SNAP solution to copper(II) sulfate solution set to pH 4 by addition of sulfuric acid following the manufacturer's instructions.

Variable Chlorophyll Fluorescence Measurements

Fluorescence Relaxation Kinetics

Flash-induced increase and the subsequent decay of chlorophyll fluorescence yield were measured by a double-modulation fluorometer (PSII) according to the method of Vass et al. (1999). The instrument contained red LEDs for both actinic (20 μs) and measuring (2.5 μs) flashes, and was used in the 150-μs to 100-s time range with pea leaf discs.

Analysis of the fluorescence relaxation kinetics was based on the widely used model of the two-electron gate (Crofts and Wraight, 1983; Diner, 1998). According to this model, the fast (few hundred microsecond) decay component reflects Q_A⁻ reoxidation via forward electron transport in centers, which contain bound PQ (in the oxidized or semireduced form) at the Q_B site before the flash. The middle (few millisecond) phase arises from Q_A⁻ reoxidation in centers, which had an empty Q_B site at the time of the flash and have to bind a PQ molecule from the PQ pool. Finally, the slow (few second) phase reflects Q_A⁻ reoxidation with the S₂ state of the water-oxidizing complex, thus causing backward electron transport via the Q_A⁻Q_B ↔ Q_AQ_B⁻ equilibrium. In certain cases a nondecaying fluorescence component is also observed, which arises from PSII centers in which Q_A⁻ has very stable or no recombination partner at the donor site. Since the relationship between fluorescence yield and the amount of Q_A⁻ is not linear, the relative Q_A⁻ concentration was estimated with Joliot's model (Joliot and Joliot, 1964), in which the value of the parameter for energy transfer between PSII units is 0.5. The fast and middle phases are generally described by exponential components. In contrast, the slow decay of Q_A⁻ via charge recombination has been shown to obey hyperbolic decay kinetics corresponding to an apparent second-order process (Vass et al., 1999). Consequently, multicomponent deconvolution of the measured curves was performed by using a fitting function with two exponential components and one hyperbolic component:

$$F_{v,corr} = A_1 \times \exp(-t/\tau_1) + A_2 \times \exp(-t/\tau_2) + A_3/(1 + t/\tau_3) + A_0$$

where $F_{v,corr}$ is the variable fluorescence yield corrected for nonlinearity, A_0 to A_3 are amplitudes, and τ_1 to τ_3 are time constants from which the half-lifetimes can be calculated as $t_{1/2} = \ln 2\tau$ for the exponential components, and $t_{1/2} = \tau$ for the hyperbolic component.

Slow Fluorescence Induction Measurements

PSII chlorophyll fluorescence of pea leaves was monitored with a PAM fluorometer (PAM-2000; Heinz Walz GmbH). After the 2-h incubation, leaf discs were dark adapted for at least 15 min for precise determination of minimal and maximal fluorescence levels in the dark (F_0 and F_m' , respectively).

F_m was obtained by exposing the leaf sample to a high intensity (8,000 μmol m⁻² s⁻¹) short pulse (0.8 s). F_v/F_m ($F_m - F_0/F_m$) was calculated according to Genty et al. (1989). Maximum fluorescence values in the light adapted state (F_m') were determined at the end of a 30-min actinic light illumination of 130 μmol m⁻² s⁻¹. After switching the actinic light off, far-red light was applied to determine the minimal level of fluorescence at steady state (F_0'). Steady-state qP ($\Delta F/F_m' - F_0'$) was determined according to the method described by Schreiber et al. (1986) where ΔF equals $F_m' - F_s$ and F_s is the steady-state fluorescence yield during actinic illumination. Φ_{PSII} ($\Delta F/F_m'$)

was determined according to Genty et al. (1989). Steady-state NPQ was calculated as: $NPQ = (F_m - F_m')/F_m'$ (Bilger and Björkman, 1990).

The relaxation kinetics of steady-state NPQ was monitored by applying saturating pulses with 60-s intervals from the end of the 30-min actinic illumination period to determine the qE component of NPQ. qE relaxes in the first 5 min of the dark relaxation period and was calculated according to Thiele and Krause (1994) as: $qE = F_m/F_m' - F_m''/F_m''$, where F_m'' is the maximum fluorescence yield in the fifth min of dark relaxation subsequent to the illumination period.

ACKNOWLEDGMENT

We thank Dr. Irma Tari for discussion and critical reading of the manuscript.

Received October 1, 2007; accepted January 23, 2008; published February 1, 2008.

LITERATURE CITED

- Bilger W, Björkman O (1990) Role of the xanthophyll cycle in photo-protection elucidated by measurements of light-induced absorbance changes, fluorescence and photosynthesis in leaves of *Hedera canariensis*. *Photosynth Res* 25: 173–185
- Crofts AR, Wraight CA (1983) The electrochemical domain of photosynthesis. *Biochim Biophys Acta* 726: 149–185
- Delledonne M (2005) NO news is good news for plants. *Curr Opin Plant Biol* 8: 390–396
- Delledonne M, Xia Y, Dixon RA, Lamb C (1998) Nitric oxide functions as a signal in plant disease resistance. *Nature* 394: 585–588
- Delledonne M, Zeier J, Marocco A, Lamb C (2001) Signal interactions between nitric oxide and reactive oxygen intermediates in the plant hypersensitive disease resistance response. *Proc Natl Acad Sci USA* 98: 13454–13459
- Diner BA (1998) Photosynthesis: molecular biology of energy capture. *Methods Enzymol* 297: 337–360
- Diner BA, Petrouleas V (1990) Formation by NO of nitrosyl adducts of redox components of the photosystem II reaction center. II: Evidence that HCO₃⁻/CO₂ binds to the acceptor-side non-heme iron. *Biochim Biophys Acta* 1015: 141–149
- Feelisch M (1998) The use of nitric oxide donors in pharmacological studies. *Naunyn Schmiedeberg's Arch Pharmacol* 358: 113–122
- Finazzi G, Johnson GN, Dall'Osto L, Joliot P, Wollman FA, Bassi R (2004) A zeaxanthin-independent nonphotochemical quenching mechanism localized in the photosystem II core complex. *Proc Natl Acad Sci USA* 101: 12375–12380
- Floryszak-Wieczorek J, Milczarek G, Arasimowicz M, Ciszewski A (2006) Do nitric oxide donors mimic endogenous NO-related response in plants? *Planta* 224: 1363–1372
- Forti G, Gerola P (1977) Inhibition of photosynthesis by azide and cyanide and the role of oxygen in photosynthesis. *Plant Physiol* 59: 859–862
- Friederich JA, Butterworth JF (1995) Sodium nitroprusside: twenty years and counting. *Anesth Analg* 81: 152–162
- Genty B, Britantais JM, Baker NR (1989) The relationship between the quantum yield of photosynthetic electron transport and quenching of chlorophyll fluorescence. *Biochim Biophys Acta* 990: 87–92
- Goussias C, Deligiannakis Y, Sanakis Y, Ioannidis N, Petrouleas V (2002) Probing subtle coordination changes in the iron-quinone complex of photosystem II during charge separation, by the use of NO. *Biochemistry* 41: 15212–15223
- Hill AC, Bennett JH (1970) Inhibition of apparent photosynthesis by nitrogen oxides. *Atmos Environ* 4: 341–348
- Joliot A, Joliot P (1964) Etude cinétique de la réaction photochimique libérant l'oxygène au cours de la photosynthèse. *C R Hebd Seances Acad Sci* 258: 4622–4625
- Jones RJ, Kildea T, Hoegh-Guldberg O (1999) PAM chlorophyll fluorometry: a new in situ technique for stress assessment in scleractinian corals, used to examine the effects of cyanide from cyanide fishing. *Mar Pollut Bull* 38: 864–874
- Kaiser WM (1979) Reversible inhibition of the Calvin cycle and activation of oxidative pentose phosphate cycle in isolated intact chloroplasts by hydrogen peroxide. *Planta* 145: 377–382

- Kern J, Loll B, Zouni A, Saenger W, Irrgang KD, Biesiadka J** (2005) Cyanobacterial photosystem II at 3.2 Å resolution—the plastoquinone binding pockets. *Photosynth Res* **84**: 153–159
- Lamattina L, García-Mata C, Graziano M, Pagnussat G** (2003) Nitric oxide: the versatility of an extensive signal molecule. *Annu Rev Plant Biol* **54**: 109–136
- Lichtenthaler HK** (1992) The Kautsky effect: 60 years of chlorophyll fluorescence induction kinetics. *Photosynthetica* **27**: 45–55
- Lum HK, Lee CH, Butt YK, Lo SC** (2005) Sodium nitroprusside affects the level of photosynthetic enzymes and glucose metabolism in *Phaseolus aureus* (mung bean). *Nitric Oxide* **12**: 220–230
- Michelet L, Zaffagnini M, Marchand C, Collin V, Decottignies P, Tsan P, Lancelin JM, Trost P, Miginiac-Maslow M, Noctor G, et al** (2005) Glutathionylation of chloroplast thioredoxin f is a redox signaling mechanism in plants. *Proc Natl Acad Sci USA* **102**: 16478–16483
- Millar AH, Day DA** (1996) Nitric oxide inhibits the cytochrome oxidase but not the alternative oxidase of plant mitochondria. *FEBS Lett* **398**: 155–158
- Neill SJ, Desikan R, Hancock JT** (2003) Nitric oxide signalling in plants. *New Phytol* **159**: 11–35
- Petrouleas V, Diner BA** (1990) Formation by NO of nitrosyl adducts of redox components of the photosystem II reaction center. I: NO binds to the acceptor-side non-heme iron. *Biochim Biophys Acta* **1015**: 131–140
- Río LA, Corpas FJ, Barroso JB** (2004) Nitric oxide and nitric oxide synthase activity in plants. *Phytochemistry* **65**: 783–792
- Sanakis Y, Goussias C, Mason RP, Petrouleas V** (1997) NO interacts with the tyrosine radical Y_D of photosystem II to form an iminoxyl radical. *Biochemistry* **36**: 1411–1417
- Schansker G, Goussias C, Petrouleas V, Rutherford AW** (2002) Reduction of the Mn cluster of the water-oxidizing enzyme by nitric oxide: formation of an S_2 state. *Biochemistry* **41**: 3057–3064
- Schreiber U, Schliwa U, Bilger W** (1986) Continuous recording of photochemical and non-photochemical chlorophyll fluorescence quenching with a new type of modulated fluorometer. *Photosynth Res* **10**: 51–62
- Singh RJ, Hogg N, Joseph J, Kalyanamaran B** (1996) Mechanism of nitric oxide release from S-nitrosothiols. *J Biol Chem* **271**: 18596–18603
- Takahashi S, Yamasaki H** (2002) Reversible inhibition of photophosphorylation in chloroplasts by nitric oxide. *FEBS Lett* **512**: 145–148
- Thiele A, Krause GH** (1994) Xanthophyll cycle and thermal energy dissipation in photosystem II: relationship between zeaxanthin formation, energy-dependent fluorescence quenching and photoinhibition. *J Plant Physiol* **144**: 324–332
- Vass I, Kirilovsky D, Etienne A-L** (1999) UV-B radiation-induced donor- and acceptor-side modifications of photosystem II in the cyanobacterium *Synechocystis* sp. PCC 6803. *Biochemistry* **38**: 12786–12794
- Wellburn AR** (1990) Why are atmospheric oxides of nitrogen usually phytotoxic and not alternative fertilizers? *New Phytol* **115**: 395–429
- Wendehenne D, Durner J, Klessig DF** (2004) Nitric oxide: a new player in plant signalling and defence responses. *Curr Opin Plant Biol* **7**: 449–455
- Wishnick M, Lane MD** (1969) Inhibition of ribulose diphosphate carboxylase by cyanide. *J Biol Chem* **244**: 55–59
- Xu CC, Li L, Kuang T** (2000) The inhibited xanthophyll cycle is responsible for the increase in sensitivity to low temperature photoinhibition in rice leaves fed with glutathione. *Photosynth Res* **65**: 107–114
- Yamasaki H** (2000) Nitrite-dependent nitric oxide production pathway: implications for involvement of active nitrogen species in photoinhibition *in vivo*. *Philos Trans R Soc Lond B Biol Sci* **355**: 1477–1488
- Yamasaki H, Shimoji H, Ohshiro Y, Sakihama Y** (2001) Inhibitory effects of nitric oxide on oxidative phosphorylation in plant mitochondria. *Nitric Oxide* **5**: 261–270
- Yang JD, Zhao HL, Zhang TH, Yun JF** (2004) Effects of exogenous nitric oxide on photochemical activity of photosystem II in potato leaf tissue under non-stress condition. *Acta Bot Sin* **46**: 1009–1014